A tight relationship between BOLD fMRI activation/deactivation and increase/decrease in single neuron responses in human association cortex

Marie-Alphée Laurent, Corentin Jacques, Xiaoqian Yan, Pauline Jurczynski, Sophie Colnat-Coulbois, Louis Maillard, Steven Le Cam, Radu Ranta, Benoit Cottereau, Laurent Koessler, et al.

A tight relationship between BOLD fMRI activation/deactivation and increase/decrease in single neuron responses in human association cortex

Marie-Alphée Laurent[a], Corentin Jacques[a], Xiaoqian Yan[b], Pauline Jurczynski[c], Sophie Colnat-Coulbois[a,d], Louis Maillard[a,e], Steven Le Cam[c], Radu Ranta[c], Benoit R. Cottereau[f], Laurent Koessler[a], Jacques Jonas[a,e], Bruno Rossion[a,e]

[a]IMoPA, CNRS, Université de Lorraine, F-54000 Nancy, France

[b]Fudan University, Institute of Science and Technology for Brain-Inspired Intelligence, 200433, Shanghai, China

[c]Université de Lorraine, CNRS, CRAN, F-54000 Nancy, France

[d]Université de Lorraine, CHRU-Nancy, Service de Neurochirurgie, F-54000 Nancy, France

[e]Université de Lorraine, CHRU-Nancy, Service de Neurologie, F-54000 Nancy, France

[f]Centre de Recherche Cerveau et Cognition, Université Toulouse 3 Paul Sabatier, CNRS, 31052 Toulouse, France

Corresponding authors:

Marie-Alphée Laurent and Bruno Rossion

marie-alphee.laurent@univ-lorraine.fr
bruno.rossion@univ-lorraine.fr

Hôpital Central, Pavillon Krug
CHRU-Nancy
29 Avenue du Maréchal de Lattre de Tassigny
54000 NANCY

Competing Interest Statement: The authors declare no competing interest.

Keywords: single neurons; fMRI; face-selectivity; intracerebral recordings; BOLD activation; BOLD deactivation

Abstract

The relationship between Blood-Oxygen-Level-Dependent (BOLD) responses in functional magnetic resonance imaging (fMRI) and increases or decreases in neural firing rate across human brain regions, especially the association cortex, remains largely unknown. Here, we contrast direct measures of neuronal activity in two adjacent brain regions of the fusiform gyrus (FG) associated with fMRI increases (lateral FG portion) or decreases (medial FG portion) of the same category-selective neural activity. In both individual brains tested across multiple recording sessions, a frequency-tagging stimulation objectively identified a substantial proportion (about 70%) of face-selective neurons. While single-units recorded in the lateral FG showed a selective increase to faces, neurons localized in the medial FG decreased spiking activity selectively to faces. Beyond a relative reduction to faces compared to non-face objects, about a third of single neurons found in the medial FG showed genuine suppression of baseline spiking activity upon presentation of a face. These observations clarify the nature of face-selective neural activity in the human brain, which can be expressed both as increases and active suppressions of spiking activity, and, more generally, shed light on the physiological basis of the fMRI signal.

Introduction

Functional magnetic resonance imaging (fMRI) has revolutionized our understanding of human brain function. While animal studies have characterized Blood-Oxygenation-Level-Dependent (BOLD) fMRI activation as a correlate of local synaptic activity (Logothetis et al., 2001; Bartolo et al., 2011), the cellular mechanisms of deactivation (negative BOLD signals) remain unknown. Since BOLD activity relies on contrasts between (two) conditions of interest, fMRI deactivations have been attributed to various causes, i.e., (relative) decreases in neuronal activity (Shmuel et al., 2006; Devor et al., 2008; Boorman et al., 2010), (relative) increases in neural activity (without concomitant compensation by cerebral blood flow (CBF) increase) (Schridde et al., 2008), or hemodynamic contributions ("blood stealing"; Harel et al., 2002). However, notwithstanding recent evidence of fMRI deactivation associated with electrocorticographic alpha power decrease in the human visual cortex (Fracasso et al., 2021), most studies have been carried out in animal models and primary sensory or motor regions. Therefore, the relationship between BOLD responses and increases or decreases in neuronal firing rate across human brain regions, especially the association cortex, remains unknown.

Here, thanks to a unique opportunity to record fMRI and spiking activity in neighboring populations of neurons of the same region of the association cortex, we shed light on the nature of the relationship between category-selective activity recorded at macroscopic and cellular scales. Specifically, two patients with refractory epilepsy (P1, P2) were implanted with hybrid macro-microelectrodes in their fusiform gyrus, a hominoid-specific cortical structure (Weiner and Zilles, 2016) that is critically involved in face recognition (Cohen et al., 2019). While microelectrodes recording single-unit activity located in the lateral portion of P1's middle fusiform gyrus (MidFG) (i.e., in cytoarchitectonic area FG4; Lorenz et al., 2017), a region known to elicit larger BOLD activity to faces than non-face objects ('Fusiform Face Area', FFA; Kanwisher et al., 1997), in P2 they fell in the medial MidFG portion (FG3), in which lower BOLD responses to faces than objects are typically observed (Pelphrey et al., 2003; Kanwisher, 2017; Gao et al., 2018). By recording face-selective neural responses both in spiking activity and fMRI signals (independent sessions) in two neighboring regions of the same brains, we tested the hypothesis of a systematic relationship between the two types of signals. In particular, we hypothesized that

fMRI deactivations to faces were associated with a majority of face-selective decreases in spiking activity.

Materials and Methods

Participants. The study included two right-handed participants (aged 23 and 46) who were patients undergoing clinical intracerebral evaluation with depth electrodes (SEEG; Talairach and Bancaud, 1973) for refractory partial epilepsy in the Epilepsy Unit of the University Hospital of Nancy, France in 2019 (P1) and 2023 (P2). The participants gave written informed consent to participate to the study (REUNIE, 2015-A01951-48), which was approved by a national ethical committee (CPP Est III, N°16.02.01).

Intracerebral recordings acquisition. Electrophysiological data were recorded from Behnke-Fried hybrid micro-macro electrodes (Ad-Tech Medical Instrument). Intracerebral depth electrodes were stereotactically implanted within the participant's brains to delineate their seizure onset zone for clinical purposes. Electrode implantation sites were determined based on non-invasive data collected during the early stages of the investigation and were verified by CT-scan fused with a pre-operative T1-weighted MRI. The present report focuses on recordings from the macro-microelectrodes, i.e., electrodes with macro-contacts modified to include 8 recording microwires and one reference, protruding about 3 to 4 mm beyond the tip of the macro-electrode (Ad-Tech Medical; see Salado et al., 2018 for details about the macroelectrode implantation procedure). The macro-microelectrodes targeted the right (P1) and the left (P2) MidFG. Although differential recordings in the same hemisphere(s) and individual brains would have been optimal, our results are unlikely to be due to differences between the two individuals or hemispheres reported, for two reasons. First, notwithstanding the right hemisphere's dominance in human face recognition (Jonas et al., 2016; Kanwisher, 2017; Gao et al., 2018), the same contrasted pattern of BOLD activation/deactivation for faces in the lateral/medial portions of the fusiform gyrus, respectively, has been systematically observed across hemispheres (Pelphrey et al., 2003; **Fig. 2**). Second, while a larger number of single-units were found for P1 than P2 recordings, the proportions of face-selective units did not differ between the two individuals.

The microwires signal was recorded at a 30 kHz sampling rate, using a 256-channel amplifier (BlackRock Microsystems), and recording activity was band-pass filtered (0.3-7500 Hz). Here we report microelectrode data recorded during 3 days (8 sequences performed in P1) and 11 days (14 sequences performed in P2). These differences across participants were due to the clinical context in which the experiment took place. Participants were tested individually and seated at 80 cm from the computer screen.

Microwires localization in the individual anatomy. The exact position of each contact from the micro-macro electrode relative to the individual brain anatomy was determined in each participant's brain by coregistrating the post-operative CT-scan with a T1-weighted MRI of the patient. The microwires coordinates were estimated at approximately 4 mm from the tip of the macroelectrode. In addition, the location of microwires relative to fMRI-defined face-selective regions was determined by having all participants perform an fMRI face localizer a few months after the SEEG procedure, using an fMRI version of the frequency-tagging paradigm providing high SNR and reliability (Gao et al., 2018). After fMRI scanning, estimated microelectrode coordinates were rendered into the T1-weighted MRI co-registered and normalized to ACPC space with the functional Z-score map, using *MRIcroGL* for visualization. The location of the microelectrodes was also defined in relation to the boundaries of the cytoarchitectonic areas FG2/FG4 and FG1/FG3 (Rosenke et al., 2017).

Stimuli. Stimuli were selected from a large pool of 200 to 218 non-face object images and 45 to 48 face images (as in e.g., Jonas et al., 2016), presented in grayscale or color sequences. Each image contained an unsegmented object or face near the center, varying significantly in size, viewpoint, lighting conditions, and background (**Fig. 1**). Images were equalized for mean pixel luminance and contrast, but low-level visual cues associated with the two categories (faces and objects) remained highly variable, naturally minimizing the contribution of low-level visual cues to the face-selective neural responses (Rossion et al., 2015).

Face localizer paradigms. A well-validated Fast Periodic Visual Stimulation (FPVS) face localizer paradigm was performed to define face-selective neural activity. Highly variable natural images of faces were embedded periodically within a

rapid 6 Hz stream of object images. In the fMRI version (from Gao et al., 2018; also, Laurent et al., 2023), mini-face blocks ("bursts") were presented for 2.167 s every 9 s to account for the sluggishness of the BOLD response (i.e., F = 1/9 = 0.111 Hz). Each mini-block consisted of a set of seven face images alternated with six non-face object images to avoid category adaptation and maximize the contrast between faces and objects (**Fig. 1A**). Each fMRI sequence lasted 405 s and contained 44 cycles of face bursts (including a 4.5 s baseline at both the beginning and end of each sequence, respectively). During intracerebral recordings, highly variable natural images of faces were inserted periodically every fifth image (i.e., face-selective frequency at 1.2 Hz = 6/5 Hz) as usually performed (**Fig. 1B**; Rossion et al., 2015; Jonas et al., 2016). A stimulation sequence lasted 70 s, including 66 s of stimulation at full contrast flanked by 2 s of fade-in and fade-out, with gradual increases and decreases in contrast, respectively. All images were presented with a sinusoidal stimulation contrast to provide a smooth transition between successive images. Participants were unaware of the periodicity of the faces. During both fMRI and intracerebral recordings, participants stared at a small black cross presented at the center of the stimuli and detected rare brief nonperiodic color changes (70-10 times per sequence for fMRI/iEEG respectively, for 500 ms) of the fixation cross (black to red). The experiments were conducted using Matlab for P1 and Java 8 for P2.

Spike sorting. Spike detection and clustering were carried out using an automatic algorithm, based on a Bayesian approach (Le Cam et al., 2023). The clusters were visually reviewed and classified into single-units (SU) and multi-units (MU) based on their spike shape, variance, inter-spike interval distribution, and the presence of a refractory period. Of all the sessions held by the two participants, 299 SU and 62 MU were identified. Across all independent sessions (i.e., recorded on different half-days), 206 SU and 39 MU were retained for analyses. Signal processing and frequency-domain analyses were similar to previous SEEG studies (Jonas et al., 2016; Hagen et al., 2020). An average of 2 units per contact were isolated.

Intracerebral recordings analyses. Analyses were performed using the free software *Letswave 6,* running on MATLAB R2022a. A Fast Fourier Transform (FFT) was applied to the iEEG recordings, and the amplitude spectrum was cut into 1 Hz

segments centered on the face-selective frequency and its three additional harmonics (i.e., 1.2 Hz, 2.4 Hz, 3.6 Hz, and 4.8 Hz), as well as on the base stimulation frequency and its harmonics (i.e., 6 Hz, 12 Hz, and 24 Hz). The amplitude of these FFT segments was summed and transformed into a Z-score. Z-scores were computed as the difference between the amplitude at the target frequency bin and the mean amplitude of 20 surrounding bins (10 on each side) divided by the standard deviation of amplitudes in the corresponding 20 bins. SNR spectra were also calculated as the ratio between the amplitude at each frequency bin and the average of the corresponding 20 surrounding bins (11 on each side, excluding the 2 bins directly adjacent to the bin of interest). A cluster (SU or MU) was considered as showing a significant response for faces and classified as "face-selective" if the Z-score at the target frequency bin exceeded 1.64 (i.e., $p < 0.05$ one-tailed). In addition, face-selectivity was characterized at a more conservative threshold (i.e., $Z > 2.32$, $p < 0.01$). To isolate face-selective responses from responses to non-face objects in the time domain (as in **Fig. 2C, F**), an FFT notch filter (filter width = 0.05 Hz) was then applied on the 70 s single or multi-units time-series to remove the general visual response at 6 Hz and two additional harmonics (i.e., 12 and 18 Hz). To account for the sinusoidal modulation of contrast, the face onset time was shifted forward by 33 ms (~1/5 of a 6 Hz cycle duration). This delay was estimated by comparing SEEG responses to sequences presented with sinewave or squarewave (i.e., abrupt) contrast modulation of visual stimulation. The onset of face-selective response was delayed by 30-35 ms for sinusoidal visual stimulation, which corresponds to 4 screen refresh frames (33 ms) and 35% of the full contrast. The spike trains of each identified cluster were then segmented into 1-s segments around face onset, and the resulting epochs were temporally smoothed (20 ms time-window) and averaged. The net average spike rate was calculated by subtracting each sequence's mean baseline spike rate in a [-0.166–0 s] time-window relative to face onset. Finally, the latency was computed as the time point at which net firing crossed the baseline +/- 2.58 s.d. value (i.e., $p < 0.01$, two-tailed percentile bootstrap) for at least 30 ms. as described in Jacques et al., 2022.

FMRI acquisition. The two participants were scanned at the CHRU-Nancy, with a 3T Siemens Magnetom Prisma system (Siemens Medical System, Erlangen, Germany) with a 64-channel head-neck coil. Anatomical images were collected

using a high-resolution T1-weighted magnetization-prepared gradient-echo image (MP-RAGE) sequence (192 sagittal slices, TR = 2300 ms, TE = 2.6 ms; flip angle (FA) = 9˚, field of view (FOV) = 256 × 256). Functional images were collected with a T2*-weighted simultaneous multi-slice echo planar imaging (SMS EPI) sequence (TR = 1500 ms, TE = 30 ms, FA = 72˚, FOV= 240×240 mm^2, voxel size = 2.5 mm isotropic, matrix size = 96×96 for sequences done in 2019 or matrix size = 80x80 for sequences done in 2022, interleaved), which acquired 44 oblique-axial slices covering the entire temporal and occipital lobes. The total duration of each sequence (run) for P1 (tested in 2019) was 333 s including 9 s of dummy scans (222 TRs). The total duration of each run for P2 (tested in 2022) was 405 s including 9 s of dummy scans (270 TRs). Images were back-projected onto a projection screen by an MRI-compatible LCD projector. The participants observed the sequences through a mirror placed within the FR head coil. The images subtended a viewing angle of 8° × 8° (33.4 cm × 33.4 cm) at a viewing distance of 240 cm. Three fMRI sequences were performed for each patient, who were scanned 6-8 weeks after the microelectrode recordings.

FMRI analyses. As in Laurent et al. (2023), the volumes of each run were first rigidly realigned with each other, and a mean functional image of the runs was computed for co-registration with the anatomical image, using *SPM12*. The volumes were also spatially smoothed with a Gaussian kernel of 2 mm (FWHM; i.e., full width at half maximum). The functional runs were averaged across runs in the volumetric space. Then, a Fourier analysis was performed using the FFT function in Matlab without windowing. The FFT was applied on the entire BOLD response time-course and the amplitude spectrum was directly derived from the Fourier transform coefficients. Amplitudes at the face stimulation frequency (i.e., at F = 0.111 Hz) were converted into Z-scores, using the mean and standard deviation of the amplitude at neighboring frequencies (see Gao et al., 2018 for details). The relative activations and deactivations of the neural responses at the face stimulation frequency were defined by the phase of the BOLD response. For each individual, the histogram (20 bins) of phase values of all the voxels with a Z-score > 3.1 and with a positive phase value was calculated. The phase value of the histogram bin that has the largest number was used as the center phase (φ) to define all the voxels with their phase values within $\varphi \pm \pi/2$ as activations (+ sign) and voxels with their phase values

outside of this window as deactivations (− sign). These signs were then applied to Z-score maps to obtain the final response map.

Results

In both MidFG regions sampled, robust differential activity to natural images of faces *vs.* non-face categories was objectively recorded with a similar well-validated frequency-tagging paradigm in fMRI (**Fig. 1A**) and microelectrode electrophysiological recordings (**Fig. 1B**).

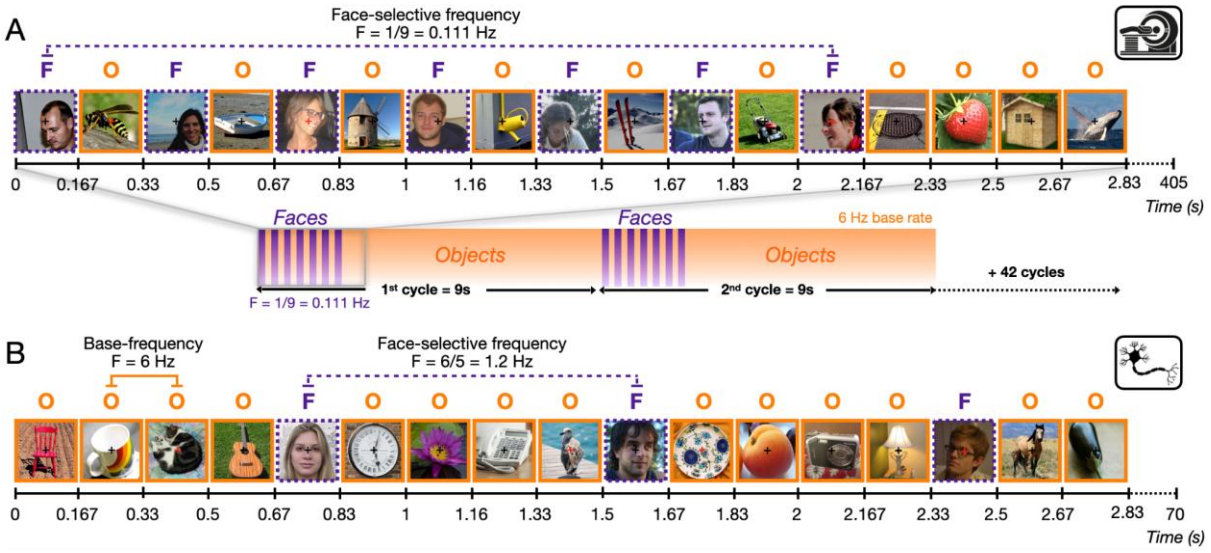

Fig. 1. The frequency-tagging Face Localizer paradigm in fMRI (Gao et al., 2018) and intracerebral electrophysiological recordings (Jonas et al., 2016). In both cases, the same variable natural non-face images alternate at a 6 Hz rate (1 fixation/image). **(A)** During a 405 s fMRI run, a "mini-burst" of 7 images of variable faces (purple: "F") alternating with 6 non-face object images (orange: "O") is presented every 9 s (0.111 Hz). A full run is composed of 44 cycles (3 s shown here). **(B)** During intracerebral recordings, variable face images are inserted periodically every fifth image (1.2 Hz). Each recording includes two 70-s stimulation sequences (3 s shown here). With both recording methods (and EEG; Rossion et al., 2015), this paradigm provides robust population-level face-selective activity devoid of low-level sensory confounds at the tagged frequencies. Here it is applied to single and multi-unit recording activity in the human fusiform gyrus.

FMRI category-selective responses

Fig. 2A and D illustrate the category-selective regions identified with fMRI, on axial, coronal, and sagittal slices in both participants (Z > 3.1; $p < 0.001$), relative to the microelectrodes location. Fast Fourier Transform (FFT) of the BOLD response time-courses is used to define face-selective voxels in the frequency-domain (0.111 Hz; Gao et al., 2018). BOLD frequency spectra at each voxel are transformed into Z-scores, which can either be positive (higher response to face than non-face stimuli, i.e., BOLD signal increase) or negative (lower response to faces than non-faces, i.e., BOLD signal decrease).

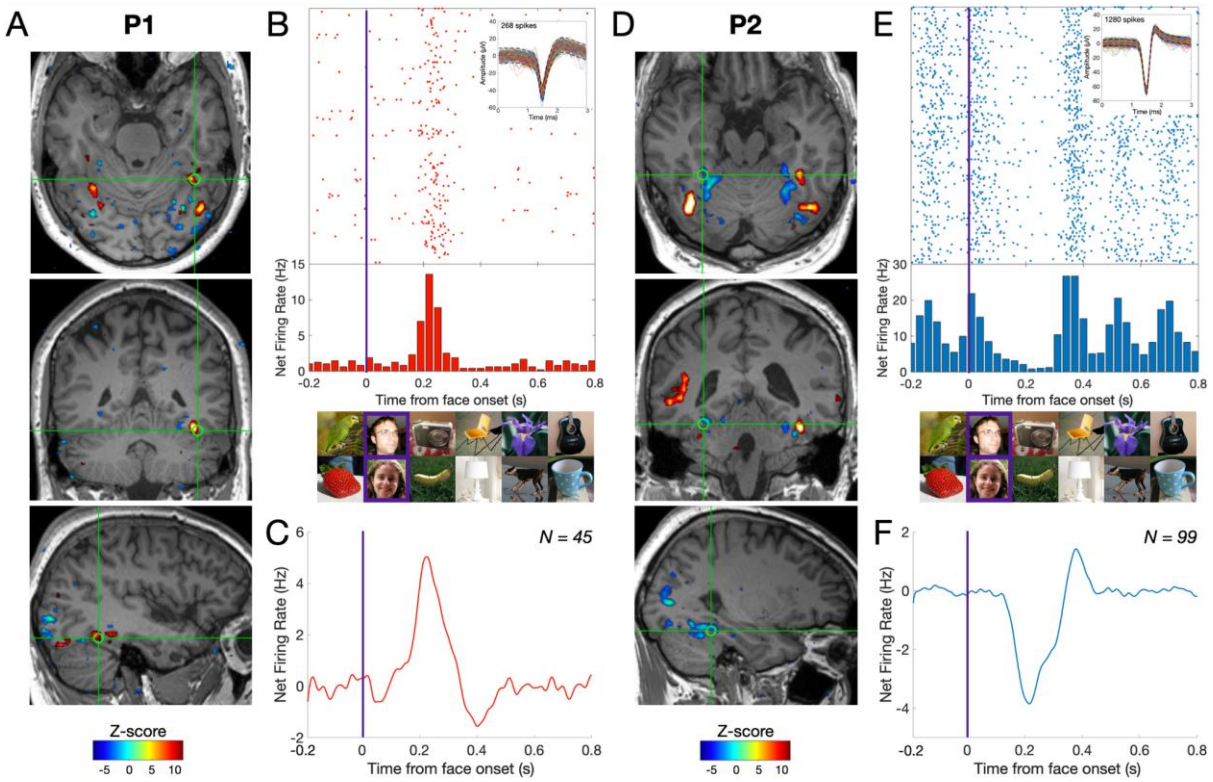

Fig. 2. Relationship between BOLD signal and neuronal activity in the human MidFG. (A), (D) Significant face-selective activations (hot colors) and deactivations (cold colors) on axial, coronal, and sagittal slices (Z > 3.1; $p < 0.001$). The estimated location of the microelectrode (green circle) falls in left MidFG activation in P1 and right MidFG deactivation in P2. **(B), (E)** Representative raster plots of two face-selective single-units (SU) showing activity increase in P1 and decrease in P2 to faces, respectively. The representative face-selective SU in panel B also exhibits a high increase in firing rate to the general visual stimulation at 6 Hz. Each line corresponds to a 1 s epoch time-locked to the onset of a face (at 0 s), from a 140 s of recording. SU waveforms are shown in the upper-right corners. **(C), (F)** Average time-courses of all face-selective SU identified (N = 45 across 4 sessions in

P1, N = 99 across 7 sessions in P2; Z > 2.32, p < 0.01), showing response increase to faces in P1 and decrease to faces in P2.

As expected, faces elicited larger BOLD responses than non-face objects in the lateral MidFG, but lower responses in the medial MidFG (Pelphrey et al., 2003; Gao et al., 2018). Microwires in P1 (estimated Talairach location -40, -46, -19; **Fig. 2A**) fell in the lateral MidFG face-selective region: the Fusiform Face Area ("FFA", peak coordinate: -35, -51, -18) (Quiroga et al., 2023), while microwires in P2 (29, -41, -12; **Fig. 2D**) located in the medial MidFG, an unprecedented sampled region with lower (deactivated) BOLD signal for faces.

Cellular category-selective responses

Recordings of category-selective spiking activity in P1 and P2 took place over up to 11 days, with single-units detected on 7 microwires per session. Across all independent sessions (i.e., on different half-days), we recorded 245 units (N = 206 single-units, SU and N = 39 multi-units, MU; pooled over 4 sessions for P1 and 7 sessions for P2) firing to variable pictures of faces and objects. Following FFT, common visual responses to faces and objects were identified at the base frequency rate and harmonics (6, 12, and 18 Hz) while face-selective responses were measured at the specific face-stimulation frequency and harmonics (i.e., 1.2, 2.4, 3.6, and 4.8 Hz; **Fig. 1B**) (Rossion et al., 2015; Jonas et al., 2016). Despite a brief recording time for each unit (2 sequences of 70 s), only a small proportion of single neurons failed to respond (i.e., no significant base rate response: N = 10/62, 16.1% in P1; N = 17/144 11.8% in P2; all Z < 1.64, all p_s < 0.05; no difference between participants, p = 0.54, Pearson's χ^2). Among all visually responsive neurons, we found a very high proportion of face-selective neurons (p < 0.05) in both activated and deactivated MidFG regions (P1: 98.1%; N = 51/52; P2: 86.6%; N = 110/127). Even at a more conservative threshold (p < 0.01), strong face-selectivity is observed (P1: 86.5%; N = 45/52 ; P2: 77.9%; N = 99/127; no difference between the two individuals, p = 0.27, Pearson's χ^2 test).

We then determined whether face-selective single neurons (p < 0.01) recorded in activated or deactivated face-selective regions exhibited different types of responses to faces relative to non-face objects. While a large majority of face-selective neurons in the lateral MidFG (P1) showed a significant relative increase in

spike rate to faces (88.9%; *N* = 40/45; **Fig. 2B, C**), most neurons in the medial MidFG (P2) showed significant relative spike rate decrease to faces (95.9%; *N* = 95/99; **Fig. 2E, F**). While the mean onset response latency did not differ between increases and decreases (118.2 ms *vs.* 127.3 ms, respectively; $p > 0.05$, two-tailed percentile bootstrap; **Fig. 2C, F**), a significantly lower response (i.e., absolute average firing rate) was found for decreases than increases ([130-300 ms]; 3.69 spikes/sec for increases, ranging from 0.99 to 7.42 spikes/sec; -2.73 spikes/sec for decreases, ranging from -0.44 to -9.67 spikes/sec; *t*-test $p < 0.01$). A final noteworthy observation is that, among the 95 single-units showing a reduced firing rate to faces (P2), 34 lacked a significant general visual response (at 6 Hz; i.e., 34,3%; $p < 0.05$). Beyond a mere relative reduction to faces compared to non-face objects, responses of such “face-exclusive” single neurons therefore appear to reflect genuine suppression of baseline spiking activity upon presentation of a face.

Discussion

Although BOLD signals correlate better with local field potentials (LFP) than spikes on a trial-by-trial basis (Logothetis et al., 2001), positive correlations have been observed between SU and BOLD in human (Mukamel et al., 2005; Nir et al., 2007) and non-human primates (Goense and Logothetis, 2008). Here thanks to a unique combination of fMRI and microelectrode recordings in the same individual human brains, we report a striking correspondence between increases/decreases in BOLD activity and (SU) neuronal firing, in two neighboring areas of the human association cortex. By showing that the sign of the BOLD signal fluctuation during visual stimulation matches the sign of SU activity, our findings shed light on the physiology of BOLD signals, revealing in particular that BOLD decreases can be due to relative, but also absolute, spike suppression in the human brain. Such transient spikes suppression could be due to suppression/reduction of synaptic inputs to the recorded neuron(s) or to inhibitory inputs to the neuron(s).

Up to now, the cellular basis of the relative BOLD decrease to faces in the medial portion of the fusiform gyrus, attributed to a smaller increase to faces relative to non-face objects or an absence of response to faces (Kanwisher, 2017), has remained somewhat of a mystery. Importantly, due to both the lack of a fusiform gyrus in non-hominoid primates (Weiner and Zilles, 2016) and of reported BOLD deactivation to faces in the monkey brain, single-unit recordings in macaque monkeys' face-selective cortical regions (Tsao et al., 2006; Bell et al., 2011) could not address this issue. Here, our neurophysiological recordings in humans suggest that faces do not only elicit a strong decrease of neuronal activity relative to non-face objects in the medial MidFG, but a genuine suppression of baseline spiking activity in a substantial proportion of the units recorded. Thus, beyond contributing to clarify the physiological basis of the fMRI signal, our study shed light on the nature of face-selective neural activity in the human brain, which can be expressed both as increase and active suppression of spiking activity. Inhibitory cellular activity is thought to play an important balancing role to maintain stable function of cortical circuits (Vogels et al., 2011), and has been shown to play a key role in cortical category-selectivity (Wang et al., 2000). Further direct recordings in the human

association cortex will be necessary to determine the functional relevance (i.e., relationship to visual recognition behavior) and the cellular mechanisms (linked to cyto- and myelo-architecture; Lorenz et al., 2017) underlying these category-selective (excitatory and) inhibitory neuronal activities.

Acknowledgments

We thank the two participants for their involvement in the study. This research was supported by the ERC Adg HumanFace 101055175 awarded to Bruno Rossion and a PhD fellowship from the Université de Lorraine to Marie-Alphée Laurent.

References

Bartolo, M. J. *et al.,* Stimulus-induced dissociation of neuronal firing rates and local field potential gamma power and its relationship to the blood oxygen level-dependent signal in macaque primary visual cortex. *Eur J. Neurosci.* **34**, 1857–1870 (2011). https://doi.org/10.1111/j.1460-9568.2011.07877.x

Bell, A. H. *et al.,* Relationship between Functional Magnetic Resonance Imaging-Identified Regions and Neuronal Category Selectivity. *J. Neurosci.* **31**, 12229–12240 (2011). https://doi.org/10.1523/JNEUROSCI.5865-10.2011

Boorman, L. *et al.,* Negative Blood Oxygen Level Dependence in the Rat:A Model for Investigating the Role of Suppression in Neurovascular Coupling. *J. Neurosci.* **30**, 4285–4294 (2010). https://doi.org/10.1523/JNEUROSCI.6063-09.2010

Cohen, A. L. *et al.,* Looking beyond the face area: Lesion network mapping of prosopagnosia. *Brain* **142**, 3975–3990 (2019). https://doi.org/10.1093/brain/awz332

Devor, A. *et al.,* Stimulus-Induced Changes in Blood Flow and 2-Deoxyglucose Uptake Dissociate in Ipsilateral Somatosensory Cortex. *J. Neurosci.* **28**, 14347–14357 (2008). https://doi.org/10.1523/jneurosci.4307-08.2008

Fracasso, A. *et al.,* FMRI and intra-cranial electrocorticography recordings in the same human subjects reveals negative BOLD signal coupled with silenced neuronal activity. *Brain Struct Funct* **227**, 1371–1384 (2022). https://doi.org/10.1007%2Fs00429-021-02342-4

Gao, X., Gentile, F. & Rossion, B. Fast periodic stimulation (FPS): a highly effective approach in fMRI brain mapping. *Brain Struct Funct* **223**, 2433–2454 (2018). https://doi.org/10.1007/s00429-018-1630-4

Goense, J. B. M., & Logothetis, N. K. Neurophysiology of the BOLD fMRI signal in awake monkeys. *Curr Biol* **18**, 631–640 (2008). https://doi.org/10.1016/j.cub.2008.03.054

Hagen, S. *et al.,* Spatially Dissociated Intracerebral Maps for Face- and House-Selective Activity in the Human Ventral Occipito-Temporal Cortex. *Cereb Cortex* **30**, 4026–4043 (2020). https://doi.org/10.1093/cercor/bhaa022

Harel, N., Lee, S.-P., Nagaoka, T., Kim, D.-S. & Kim, S.-G. Origin of negative blood oxygenation level-dependent fMRI signals. *J Cereb Blood Flow Metab* **22**, 908–917 (2002). https://doi.org/10.1097/00004647-200208000-00002

Jacques, C. *et al.,* Low and high frequency intracranial neural signals match in the human associative cortex. *ELife* **11**, 76544 (2022). https://doi.org/10.7554/eLife.76544

Jonas, J. *et al.,* A face-selective ventral occipito-temporal map of the human brain with intracerebral potentials. *Proc. Natl. Acad. Sci. USA* **113** E4088–E4097 (2016). https://doi.org/10.1073/pnas.1522033113

Kanwisher, N. The Quest for the FFA and Where It Led. *J. Neurosci.* **37**, 1056–1061 (2017). https://doi.org/10.1523/JNEUROSCI.1706-16.2016

Laurent, M.-A. *et al.,* Towards an optimization of functional localizers in non-human primate neuroimaging with (fMRI) frequency-tagging. *Neuroimage* **270**, 119959 (2023). https://doi.org/10.1016/j.neuroimage.2023.119959

Le Cam, S. *et al.,* A Bayesian approach for simultaneous spike/LFP separation and spike sorting. *J Neural Eng* **20**, 026027 (2023). https://doi.org/10.1088/1741-2552/acc210

Logothetis, N. K., Pauls, J., Augath, M., Trinath, T. & Oeltermann, A. Neurophysiological investigation of the basis of the fMRI signal. *Nature* **412**, 150–157 (2001). https://doi.org/10.1038/35084005

Lorenz, S. *et al.* Two New Cytoarchitectonic Areas on the Human Mid-Fusiform Gyrus. *Cereb. Cortex* **27**, 373–385 (2017). https://doi.org/10.1093/cercor/bhv225

Mukamel, R., Gelbard, H., Arieli, A., Hasson, U., Fried, I., & Malach, R. (2005). Coupling between neuronal firing, field potentials, and FMRI in human auditory cortex. *Science*, *309*(5736), 951–954. https://doi.org/10.1126/science.1110913

Nir, Y., Fisch, L., Mukamel, R., Gelbard-Sagiv, H., Arieli, A., Fried, I., & Malach, R. Coupling between neuronal firing rate, gamma LFP, and BOLD fMRI is related to interneuronal correlations. *Current Biology* **17**, 1275–1285 (2007). https://doi.org/10.1016/j.cub.2007.06.066

Pelphrey, K. A., Mack, P. B., Song, A., Güzeldere, G., & McCarthy, G. Faces evoke spatially differentiated patterns of BOLD activation and deactivation. *Neuroreport* **14**, 955–959 (2003).
https://doi.org/10.1097/01.wnr.0000074345.81633.ad

Quian Quiroga, R. *et al.,* Single neuron responses underlying face recognition in the human midfusiform face-selective cortex. *Nat Commun* **14**, 5661 (2023). https://doi.org/10.1038/s41467-023-41323-5

Rosenke, M. *et al.,* A cross-validated cytoarchitectonic atlas of the human ventral visual stream. *Neuroimage* **170**, 257-270 (2017). https://doi.org/10.1016/j.neuroimage.2017.02.040

Rossion, B., Torfs, K., Jacques, C. & Liu-Shuang, J. Fast periodic presentation of natural images reveals a robust face-selective electrophysiological response in the human brain. *J Vis* **15**, 18–18 (2015). https://doi.org/10.1167/15.1.18

Salado, A. L. *et al.,* sEEG is a Safe Procedure for a Comprehensive Anatomic Exploration of the Insula: A Retrospective Study of 108 Procedures Representing 254 Transopercular Insular Electrodes. *Oper Neurosurg (Hagerstown)* **14**, 1–8 (2018). https://doi.org/10.1093/ons/opx106

Schridde, U. *et al.,* Negative BOLD with Large Increases in Neuronal Activity. *Cereb Cortex* **18**, 1814–1827 (2008). https://doi.org/10.1093%2Fcercor%2Fbhm208

Shmuel, A., Augath, M., Oeltermann, A. & Logothetis, N. K. Negative functional MRI response correlates with decreases in neuronal activity in monkey visual area V1. *Nat Neurosci* **9**, 569–577 (2006). https://doi.org/10.1038/nn1675

Talairach, J. & Bencaud, J. Stereotaxic approach to epilepsy: methodology of anatomo-functional stereotaxic investigations. *Prog Neurol* **5**, 1-67 (1973). https://doi.org/10.1159/000394343

Tsao, D. Y., Freiwald, W. A., Tootell, R. B. H. & Livingstone, M. S. A Cortical Region Consisting Entirely of Face-Selective Cells. *Science* **311**, 670–674 (2006). https://doi.org/10.1126/science.1119983

Vogels, T. P., Sprekeler, H., Zenke, F., Clopath, C., & Gerstner, W. Inhibitory plasticity balances excitation and inhibition in sensory pathways and memory networks. *Science* **334**, 1569–1573 (2011). https://doi.org/10.1126/science.1211095

Wang, Y., Fujita, I., & Murayama, Y. Neuronal mechanisms of selectivity for object features revealed by blocking inhibition in inferotemporal cortex. *Nature neuroscience* **3**, 807–813 (2000). https://doi.org/10.1038/77712

Weiner, K. S. & Zilles, K. The anatomical and functional specialization of the fusiform gyrus. *Neuropsychologia* **83**, 48–62 (2016). https://doi.org/10.1016/j.neuropsychologia.2015.06.033